Toxic Effects of Thioacetamide-Induced Femoral Damage in New Zealand White Rabbits by Activating the p38/ERK Signaling Pathway

Linyan CHENG[1#], Yang LI[2#], Yetao YAO[1], Xiaoli JIN[1], Hang YING[1], Bin XU[3], Jian XU[1]
[#]*These authors contributed equally to this work*

[1]School of Medical Technology and Information Engineering, Zhejiang Chinese Medical University, Hangzhou, Zhejiang, China, [2]School of basic medical sciences, FUDAN University, Shanghai, China, [3]Department of General Surgery, Sir Run Run Shaw Hospital, School of Medicine, Zhejiang University, Hangzhou, Zhejiang, China

Received September 13, 2021
Accepted February 18, 2022
Epub Ahead of Print March 11, 2022

Summary

Thioacetamide (TAA) is widely used in the production of drugs, pesticides and dyeing auxiliaries. Moreover, it is a chemical that can cause liver damage and cancer. TAA has recently been identified to cause bone damage in animal models. However, the type of bone damage that TAA causes and its potential pathogenic mechanisms remain unclear. The toxic effects of TAA on the femurs of New Zealand white rabbits and the underlying toxicity mechanism were investigated in this study. Serum samples, the heart, liver, kidney and femurs were collected from rabbits after intraperitoneal injection of TAA for 5 months (100 and 200 mg/kg). The New Zealand white rabbits treated with TAA showed significant weight loss and femoral shortening. The activities of total bilirubin, total bile acid and gamma-glutamyl transpeptidase in the serum were increased following treatment with TAA. In addition, the cortical bone became thinner, and the trabecular thickness decreased significantly in TAA-treated rabbits, which was accompanied by significantly decreased mineral density of the cortical and trabecular bone. Moreover, there was a significant decrease in modulus of elasticity and maximum load on bone stress in TAA-treated rabbits. The western blotting results showed that the expression of phosphorylated (p)-p38 and p-ERK in femur tissues of rabbits were increased after TAA administration. Collectively, these results suggested that TAA may lead to femoral damage in rabbits by activating the p38/ERK signaling pathway.

Key words

Thioacetamide • Toxicity • Bone damage • MAPKs • Micro-CT

Corresponding author

Jian Xu, School of Medical Technology and Information Engineering, Zhejiang, Chinese Medical University, Hangzhou, Zhejiang 310053, P.R. China. E-mail: xujian832002@163.com, Bin Xu, Department of General Surgery, Sir Run Run Shaw Hospital, School of Medicine, Zhejiang University, Hangzhou, Zhejiang 310016, P.R. China. E-mail: 3304089@zju.edu.cn

Introduction

Thioacetamide (TAA; C_2H_5NS) is an organo-sulfur that has been found to induce liver damage and cancer, and it is often used in experimental animal models to induce liver fibrosis [1,2]. TAA undergoes a two-step bioactivation to TAA sulphoxide, then the active metabolite TAA-S, S-dioxide ($TASO_2$) [3]. $TASO_2$ binds to other molecules responsible for altering cell permeability and the movement of calcium ions in and out of the cell. The disruption of the calcium balance between the inside and outside of the cell eventually leads to cell death [4]. The conversion between TAA sulfides promotes the production of numerous reactive oxygen species (ROS), which ultimately hinder the antioxidant mechanisms in the body and damage cell structure and function [5].

TAA has been identified to cause bone damage in animal models. As early as 1984, Pauli Virtanen and Veijo Lassila identified that osteoclastic bone resorption was increased in the alveolar crest and there was

sustained calcium^{+} deficiency in the horizontal bone after female rats were administered a daily injection of TAA [6]. Nakano A *et al*. also observed that the bone volume of cirrhotic rats treated with thioacetamide was significantly reduced, and resulting in osteoporosis due to the combination of low bone formation rate and high bone resorption rate [7]. Moreover, examination of mouse bone marrow using the micronucleus test activity suggested that TAA was a genotoxic carcinogen [8]. However, since then, there have been few studies on the bone damage caused by TAA, to the best of our knowledge, and most of the research has focused on the injury to the liver, kidney and brain [9-11].

Osteoporosis is considered to be one of the major epidemics of the 21st century, affecting ~200 million individuals worldwide, with significant morbidity and mortality rates [12]. Osteoporosis is characterized by a loss of bone tissue area and bone mass. Specifically, it is an imbalance in the activities of osteoblasts and osteoclasts, which increases bone brittleness and causes a higher risk of fractures to the bone[13]. Osteoporosis significantly increases the risk of short height, a hump-like appearance, back pain and even fractures, which seriously endangers and affects the quality of life, bringing heavy burdens to patients and society [14].

The adult skeleton is continuously reshaped to maintain bone integrity and bone homeostasis via the strict regulation of bone resorption and formation [15]. The receptor activator of NF-κB ligand (RANKL) and the receptor of RANKL form a critical upstream signaling pathway involved in osteoclast formation, which triggers various downstream signaling transduction pathways, such as those involving MAPKs and Akt, ultimately stimulating the activation of key genes involved in osteoclast formation [16]. Phosphorylated-ERK (p)-ERK is a key regulator of the activation of activator protein 1 (AP-1) in bone marrow macrophages [17]. p-p38 is important in the differentiation of osteoclasts, because it can promote the expression of tartrate-resistant acid phosphatase (TRAP) [18]. In addition, bone morphogenetic protein 2 (BMP2) is a major contributor to postnatal bone homeostasis. The lack of BMP2 hinders the development of bone progenitor cells into bone cells, and BMP2 provides osteogenic signals that are essential for the intrinsic repair of bone [19]. Therefore, these proteins serve important roles in regulating homeostasis balance and maintaining skeletal integrity.

Overall, it has been reported that TAA may cause new bone toxicity, in addition to liver and kidney damage, which may overcome the stereotype of TAA toxicity [7,8,20]. Although TAA is toxic to various organs and also carcinogenic, it was widely used for the synthesis of multiple clinical drugs [21,22]. It was also widely used in the synthesis of chemical materials, electroplating, pesticide synthesis and hair dye [23-25]. Therefore, more attention needs to be paid to the damage caused by TAA, it is supposed that TAA can cause bone damage similar to osteoporosis. In addition, rabbits are more suitable for the study of osteoporosis because of their body size, haversian remodelling and closure of epiphyseal plate[26]. In this study, we aimed to investigate the bone toxicity induced by TAA and the mechanism of action in New Zealand white rabbits.

Methods

Animals and treatment

TAA (purity >98 %) was obtained from Sangon Biotech Co., Ltd. (Shanghai, China). In this study, 36 healthy male New Zealand white rabbits (2.5-3.0 kg, 14 weeks) were purchased from Xinchang County, Dashi Town Xin Jian rabbit farm (Zhejiang, China, certificate no.: SCXK 2015-0004). All the rabbits were housed in clean metal cages in The Animal Experimental Research Center of Zhejiang Chinese Medical University. The animals were kept at 20±2 °C and 50±10 % humidity with free access to food and water in a 12-hour light/dark cycle. The rabbits were randomly divided into the control group (n=12), low-dose group (100 mg/kg, n=12) and high-dose group (200 mg/kg, n=12), the control group was intraperitoneally injected with normal saline. Rabbits were intraperitoneally injected once every 2 days for 20 weeks. The weight was recorded before and after the experiment. All procedures involving animals were performed under the National Institutes of Health Guidelines for the Care and Use of Laboratory Animals. The present study was approved by The Animal Ethical and Welfare Committee of Zhejiang Chinese Medical University (approval no. IACUC-20181029-02).

Serum biochemical analysis

Venous blood was collected from rabbits (2-3 ml only), and the serum was obtained by centrifugation (1,500 × g for 15 min at 4 °C). The activities of alanine aminotransferase (ALT), aspartate aminotransferase (AST), total bilirubin (TBIL), bile acid (TBA), gamma-glutamyl transpeptidase (GGT) and cholinesterase (ChE)

in the serum were analyzed using a Roche analyzer (Roche, Basel, Switzerland).

HE, Masson and TRAP staining

The rabbits were anesthetized with an intravenous injection of 3 % pentobarbital (100 mg/kg) and sacrificed by exsanguination. The femur, liver, kidney and heart were removed after the euthanasia of the rabbits, and the length of the femur was measured. These tissues were firstly immersed in 10 % formalin for 24 h. The femur tissue was immersed in decalcification solution for 8 weeks, dehydrated in gradient ethanol, and then deparaffinized in xylene, dipped in the wax and made into tissue wax block. Paraffin slices of a thickness of 4 μm were used with HE, Masson and TRAP staining (Jiancheng Bioengineering Institute, Nanjing, China), and then examined for pathological changes under an optical microscope RX50 (Ningbo Sunny Instruments Co., Ltd., magnification x200).

Micro-CT analysis

Muscle and attachment tissue were removed from the left femur, and the femur was placed into a Micro-CT SkyScan 1176 (Bruker, Karlsruhe, Germany) for X-ray scanning (voltage 90 kV, current 260 μA). Then, the scanned area of interest (ROI) from the micro-CT system was selected to analyze the microstructure of the femur. The test results of trabecular thickness (Tb.Th), bone volume/tissue volume fraction (BV/TV, the ratio of bone tissue volume to tissue volume, directly reflect the change of bone mass)=, structure model index (SMI) and bone mineral density (BMD) were collected. SMI is a parameter that describes the ratio of rod-to-lamellar structures in the structural composition of trabecular bone. The more rod-like trabecular bone, the greater the SMI.

Three-point bending test

Biomechanical strength was examined with an Electronic universal testing machine (Instron, Massachusetts, USA). The right femur was tested for three-points bending test; the span was set at 5 cm, and the load was set at 5 mm/min. The load-deformation curve was recorded, and the maximum load and elastic modulus were determined with a calculation according to the load-deformation curve.

Western blot analysis

The femoral head samples were milled and lysed with RIPA lysis buffer for extracting total proteins. Each sample was separated via 10 % SDS-PAGE, and transferred to polyvinylidene difluoride (PVDF) membranes. The membrane transfer conditions were 1.5 h and 200 mA. The membranes were then blocked with 5 % skimmed milk in TBS-Tween 20 (TBST, 0.1 % Tween 20) buffer, rinsed three times with TBST, and then incubated with antibodies targeting β-actin (1:5000, Abcam, Cambridge, England), Runx2 (1:1000), BMP2 (1:1000), p38 (1:1000), p-p38 (1:1000), ERK (1:1000) and p-ERK (1:1000, Bioss, Beijing, China) overnight at 4°C. After washing with TBST, the membranes were incubated with the secondary antibody of IgG (1:5000, Abcam, Cambridge, England) for 2 h. Finally, the protein bands were analyzed using ImageJ 1.8.0 software (National Institutes of Health).

Statistical analysis

In this study, all data are presented as the mean ± standard deviation (x ± S). One-way analysis of variance (ANOVA) coupled with a post hoc analysis was used to determine statistical differences of multi-groups. All the data were analyzed using SPSS 25.0 software (IBM Corp.). $P<0.05$ was considered to indicate a statistically significant difference.

Results

TAA affects the growth of New Zealand white rabbits

The body weight of the New Zealand white rabbits after treatment with TAA was significantly decreased by the end of the experiment, especially in the high-dose group (Fig. 1A). Moreover, in terms of weight changes (Weight changes = final weight - initial weight), there were significant differences between the rabbits in the TAA and control groups. After 20 weeks of intraperitoneal injection with TAA, the New Zealand white rabbits demonstrated a significantly decreased body weight. In addition, the high-dose group lost more weight compared with the low-dose group (Fig. 1B). Femurs in rabbits treated with TAA were significantly shorter, especially in the high-dose group, which appeared to be shorter and narrower at the same time (Fig. 1C and 1D), but it may be partly affected by weight loss.

TAA increases the activity of TBIL, TBA and GGT in serum

No significant increases were observed in ALT, AST and ChE between the rabbits after treatment with TAA and the control group (data not shown).

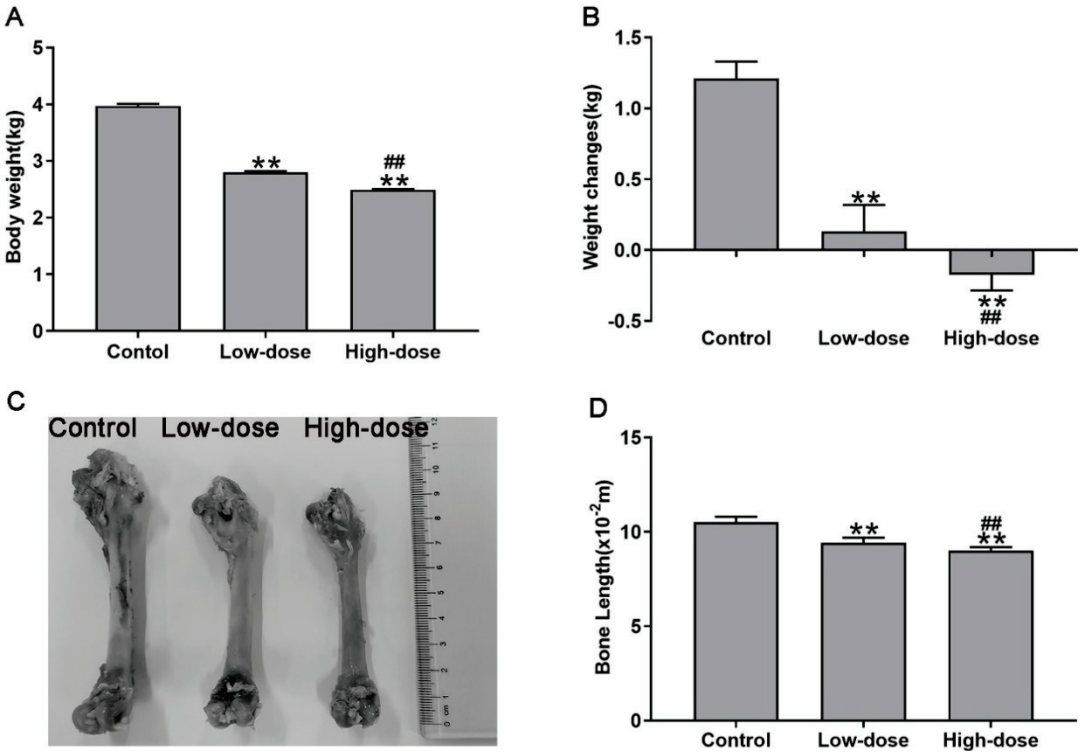

Fig. 1. Effects of TAA on the femur and body weight of the New Zealand white rabbits. (**A**) Weight of rabbits in each group at week 20. (**B**) Weight change (week 20- week 0) of rabbits in each group. (**C**) Images of the left femurs in each group. (**D**) Femoral length of each group. ***P*<0.01 vs. control. ##*P*<0.01 vs. low-dose. TAA, Thioacetamide.

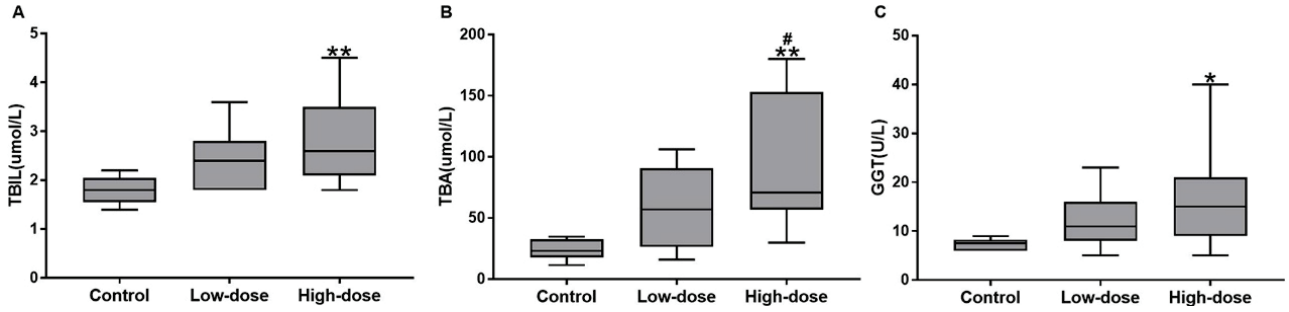

Fig. 2. Effects of TAA on serum TBIL, TBA and GGT activities. **P*<0.05, ***P*<0.01 vs. control. #*P*<0.05 vs. low-dose. TAA, Thioacetamide; TBIL, total bilirubin; TBA, bile acid; GGT, beta-glutamyl transpeptidase.

Furthermore, compared with the control group, only the activities of TBIL, TBA and GGT were increased in the New Zealand white rabbits after treatment with TAA for 20 weeks. There were significant differences in the TBIL activities between the high-dose group and the control group (Fig. 2A). The activity of TBA was increased in the rabbits after treatment with TAA compared with the control group (Fig. 2B). Moreover, the activity of GGT in the high-dose group was higher compared with the control group (Fig. 2C).

Fibrosis of heart, liver, and kidney was increased, as well as bone resorption after TAA treatment

Histopathological analysis revealed that the heart tissue showed only mild cardiomyocyte disturbance in New Zealand white rabbits after TAA intraperitoneal injection in the HE-stained tissue. In the liver tissue, it was identified that the hepatic lobule structure was disordered, liver cells were swollen, there were many inflammatory cells present and the boundary of the hepatic lobule was not clear. In the kidney tissue, it was found that the periglomerular lacunae were widened and there were many inflammatory cells present. In the femoral tissue, compared with the control group, the bone trabecular become sparse and thinner, even resulting in widened inter trabecular spaces, and the trabecular were unevenly colored and irregularly arranged (Fig. 3A and 3E). After the tissue was stained with Masson, collagen

deposition fibrosis in the liver, kidney and heart was observed in the rabbits after treatment with TAA, and this was most obvious in the liver (Fig. 3B). In the control group, the Haversian canals were small, smooth and neat, and significantly enlarged in the low-dose and high-dose groups (Fig. 3C). TRAP staining results of the femoral tissue showed that TRAP staining was not positive in the control group, but that there were numerous positive regions after treatment with TAA, especially in the high-dose group (Fig. 3D and 3E).

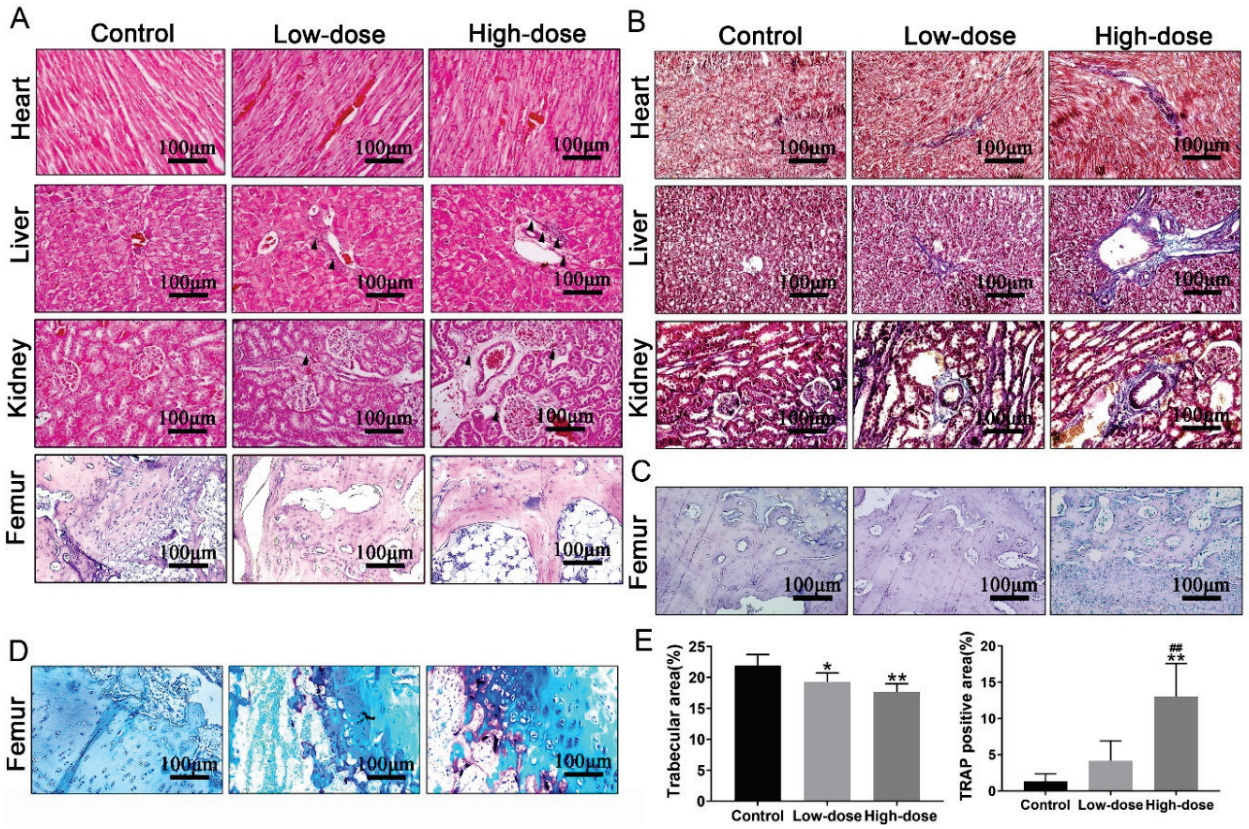

Fig. 3. Histopathological changes in the heart, liver, kidney and femur after intraperitoneal TAA administration. (**A**) HE staining; (**B**) Masson staining; (**C**) Haversian system of the femur cross-section stained with HE (**D**) TRAP staining, purplish red areas show positive TRAP expression; (**E**) Quantitative analysis of bone tissue staining. Scale bar, 100 μm. **P*<0.05, ***P*<0.01 vs. control. ##*P*<0.01 vs. low-dose. "▲" represents the inflammatory cells. TAA, Thioacetamide; HE, hematoxylin and eosin; TRAP, Tartrate-resistant acid phosphatase.

TAA damages the cortical and trabecular bone

Micro-CT was used to detect the changes in the femoral head microstructure. It was shown that the cortical bone was destroyed in the rabbits after treatment with TAA, but that the trabecular number appeared to increase in the high-dose group (Fig. 4A and 4B). TAA could decrease BV/TV and BMD in the cortical bone, especially in the high-dose group, which showed significant changes while compared with control group. Significant changes in bone mineral BV/TV, Tb.Th, SMI and BMD were also found in trabecular bone of TAA-treated rabbits; SMI were increased, while the Tb.Th was decreased, with more obvious effects observed in the high-dose group (Fig. 4C).

TAA decreases bone stress

The load-deformation curves were obtained using a three-point bending test of each groups. Compared with the control group, significant decreases in the elastic modulus and maximum load were found in the rabbits after treatment with TAA. Moreover, compared with the low-dose group, the elastic modulus was significantly decreased in the high-dose group (Fig. 5A). Similarly, there was also a significant decrease and dose-dependent relationship in the maximum load (Fig. 5B).

TAA causes an imbalance in bone-related protein expression

To investigate whether MAPKs and BMP signaling pathways are involved in TAA-induced femoral damage, the expression levels of related proteins were analyzed *via* western blot analysis. The results showed that TAA promoted the expression of BMP2 and Runx2

proteins in the femoral of rabbits compared with control group, and the protein expression of Runx2 was increased especially in the high-dose group. In addition, the protein expression levels of p-p38 and p-ERK were increased; p-ERK expression was found to be increased in a dose-dependent manner (Fig. 6A and 6B).

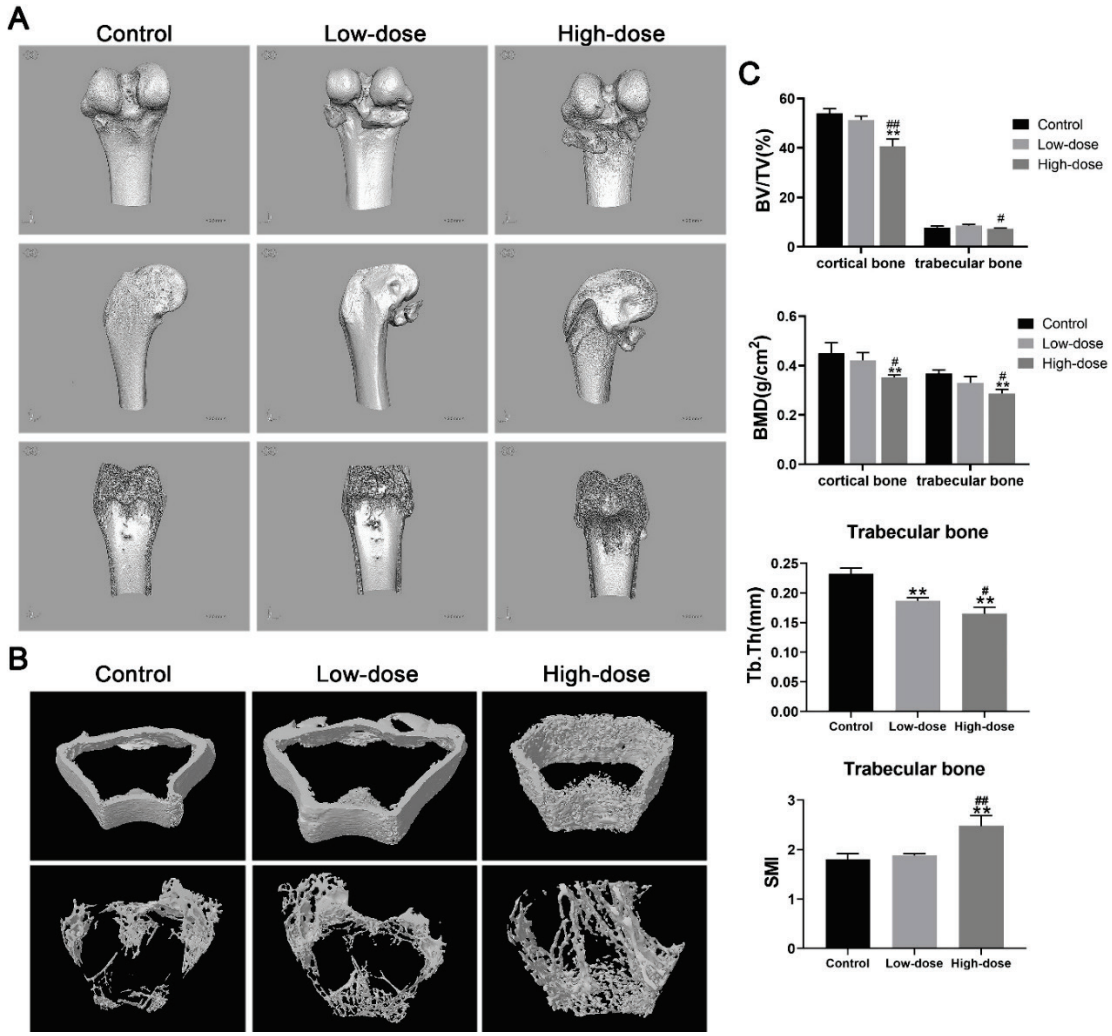

Fig. 4. Micro-CT images and corresponding quantitative results of bone microarchitecture in femurs. (**A**) Three-dimensional image for micro-CT. (**B**) Reconstruction image of cortical and trabecular bone. (**C**) Morphological parameters in the cortical and trabecular bone. **P*<0.05, ***P*<0.01 vs. control. #*P*<0.05 and ##*P*<0.01 vs. low-dose. BV, bone volume; TV, total volume; BMD, bone mineral density; Tb.Th, trabecular thickness; SMI, Structure model index.

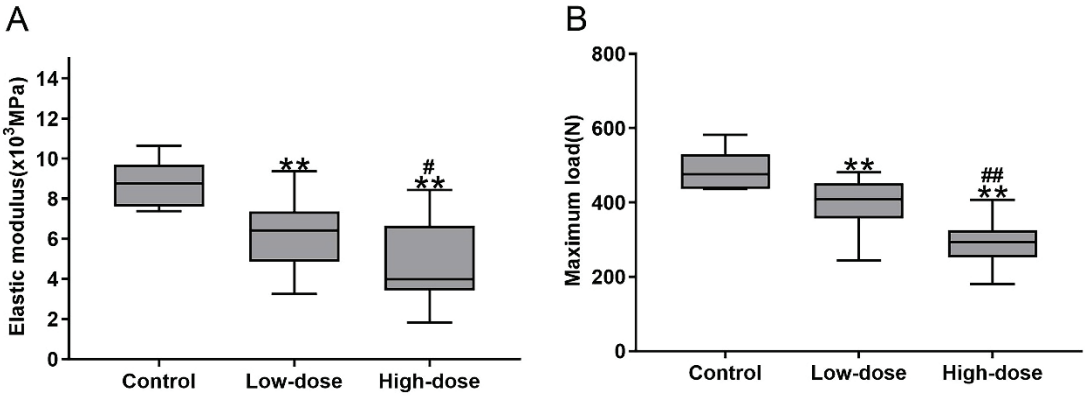

Fig. 5. Effect of TAA on bone stress in New Zealand white rabbits. (**A**) The level of the modulus of elasticity. (**B**) The level of the maximum load. ***P*<0.01 vs. control. #*P*<0.05, ##*P*<0.01 vs. low-dose. TAA, Thioacetamide.

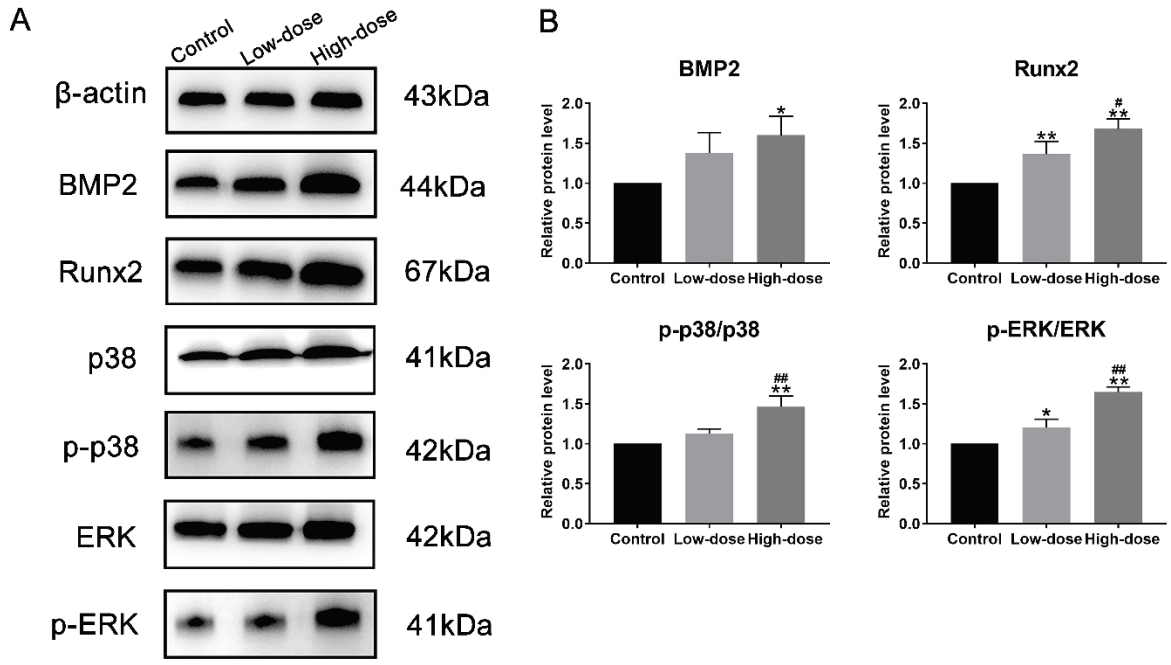

Fig. 6. TAA promotes the expression of MAPKs and BMP pathways. (**A**) The expression of the MAPKs and BMP pathways in femoral tissue of New Zealand white rabbits. (**B**) Gray value analysis of the protein of the MAPKs and BMP pathways. **P*<0.05, ***P*<0.01 vs. control. #*P*<0.05, ##*P*<0.01 vs. low-dose. BMP, bone morphogenetic protein; p-, phosphorylated; Runx2, runt-related transcription factor 2.

Discussion

As key intermediates in organic synthesis, thioamides have important biological and pharmaceutical activities and are widely used in industry, having become a commercial chemical [27,28]. The TAA-induced animal model is often used to study liver fibrosis. Prolonged exposure to TAA causes cell damage similar to human liver fibrosis [29]. The metabolism of TAA causes oxidative damage to the liver [30], and so, TAA can induce the markers of liver injury (ALT, AST, GGT), kidney function parameters (creatinine, urea, uric acid), inflammation and increase oxidative stress (antioxidant enzyme, lipid peroxidation, malondialdehyde), resulting in liver, kidney and brain damage in rats [31-33]. However, studies examining the bone damage caused by TAA are lacking, except for some early findings.

Hepatic fibrosis induced by TAA is characterized by the increased presence of inflammatory cells and oxidative stress in rats [34]. In this study, Liver injury related parameters, including serum ALT, AST, ChE, TBIL, TBA and GGT activities were measured, and only the activities of TBIL, TBA and GGT, which are involved in cholestasis, were significantly increased. The lack of changes in ALT, AST and ChE indicated that there was no more damage in the liver cells at week 20. Serum ALT, AST, TBIL, DBIL and GGT activities were found to be significantly elevated in TAA-treated rats [35]. Furthermore, cell necrosis and collagen deposition in multiple tissues were enhanced in the rabbits after treatment with TAA, especially in the high-dose group, according to histopathological findings of HE and Masson staining. Treatment with TAA causes extensive vacuolation and inflammatory cell infiltration in Wistar rat hepatocytes [36]. Ovariectomized (OVX)/TAA treated SD rats also showed increased hepatocyte necrosis and infiltration [35]. In the case of exposure to TAA, extensive hepatocyte apoptosis leads to liver fibrosis, while ROS release triggers inflammation and further aggravates cell apoptosis [37].

To assess the association between TAA and bone, bone-related experiments were performed. Weight loss occurred in TAA-treated rabbits [38]. In the present study, TAA induced femur shortening and weight loss in rabbits. Growth and development were affected by TAA, thus resulting in weight loss, including femoral shortening. Pathological staining identified that the Haversian canals were dilated, the trabecular space and osteoclasts were increased in the New Zealand white rabbits after TAA administration. The histological findings of osteoporosis are thinning of the cortical bone, enlargement of the Haversian canal, and reduction of trabecular bone [39]. The Haversian canal is a major component of compact bone substance and can be

significantly enlarged due to bone absorption in osteoporosis [40]. These results suggest that TAA inhibits the normal growth of New Zealand white rabbits and promotes bone resorption in the femur.

To date, the common clinical indicators used to diagnose osteoporosis are the occurrence of brittle fracture or loss of bone density, therefore, BMD is an important indicator of osteoporosis [41]. In this study, images of the micro-CT showed that the cortical bone was damaged and thinned after treated with TAA. Moreover, bone analysis parameters such as BV/TV and BMD of the cortical bone were decreased. With regards to the trabecular bone, BV/TV, BMD and Tb.Th were decreased and the SMI was increased, indicating that TAA reduced the lamellar structure of trabecular bone. These effects were more evident in the high-dose group. A study of Andreas K. Nussler *et al.* reported that the BMD, bone volume, trabecular number and trabecular thickness decreased significantly in CCl4-treated mice [42]. Moreover, the data observed from the bone stress detection of the femur in rabbits were consistent with the results of BMD. It was found that the maximum load and modulus of elasticity were significantly reduced in the femur of the rabbits after TAA treatment, especially in the high-dose group. Therefore, it was concluded that along with liver and kidney damage, TAA can also cause damage in the femur, and this occurs in both cortical and trabecular bones.

Runx2 is expressed early as a major regulator of bone formation, serves a role at the intersection of numerous osteogenesis-related pathways, such as the BMP signaling pathway [43]. Bone homeostasis in the adult skeleton is established by the balance between osteoclasts and osteoblasts [44]. Runx2 and BMP2, during osteoblast differentiation were significantly upregulated in animal femoral tissue after TAA treatment, which may be due to the imbalance of bone homeostasis caused by TAA. BMP2 plays important roles in bone remodeling and homeostasis in adults, and bone remodeling occurs in adults with osteoporosis [45]. RANKL can induce the activation of MAPKs, such as p38, ERK and JNK, to promote the formation of murine osteoclasts [46]. A study by Youn-Hwan Hwang *et al*. revealed that persimmon leaves have anti-osteoporosis effects by inhibiting the protein expression of MAPKs in OVX-induced bone loss mice [47]. In this study, the protein expression of p-p38 and p-ERK were significantly increased in animal femoral tissues after TAA treatment. This suggests that TAA-induced femoral damage may be associated with the promotion of p38 activation and ERK signaling.

TAA-induced bone damage includes the decreased formation of new alveolar bone in rats [48]. Moreover, the increase in micronucleated polychromatic erythrocytes following TAA treatment suggests that TAA is a genotoxic carcinogen, and the bone volume in TAA-treated cirrhotic rats is significantly decreased [7, 8]. In the current study, New Zealand white rabbits treated with TAA at different doses were found to have severely damaged femoral cortical and trabecular bones, which may result in osteoporosis. Furthermore, the effects of TAA were observed to occur in a dose-dependent manner. The present results also suggested that TAA promotes osteoclast differentiation to some extent by activating p38/ERK signaling pathways, while bone remodeling after bone injury is mediated by the upregulation of the BMP signaling pathways. In addition, the findings of the present study indicated that TAA may be directly or indirectly associated with bone loss, weight loss, and fibrosis of the heart, liver and kidneys, which will be further investigated in subsequent studies.

In conclusion, TAA-treated New Zealand white rabbits suffered heart, liver and kidney tissue damage, and their growth and development were inhibited. Furthermore, TAA caused femoral damage in New Zealand white rabbits, including in the cortical bone and trabecular bone in the femur. The underlying mechanism of the induction of femoral damage may be that TAA enhances bone resorption in the femur of New Zealand white rabbits. Moreover, TAA may cause femoral damage via the p38/ERK signaling pathway.

Conflict of Interest

There is no conflict of interest.

Acknowledgements

This study was supported by the Natural Science Foundation of Zhejiang Province (grant no. LY19H060001) and the Zhejiang University Student Science and Technology Innovation Activity Plan (grant nos. 2019R410031 and 2020R410056).

References

1. Ichimura R, Mizukami S, Takahashi M, Taniai E, Kemmochi S, Mitsumori K, Shibutani M. Disruption of Smad-dependent signaling for growth of GST-P-positive lesions from the early stage in a rat two-stage hepatocarcinogenesis model. Toxicol Appl Pharmacol. 2010;246:128-140. https://doi.org/10.1016/j.taap.2010.04.016
2. Lebda MA, Sadek KM, Abouzed TK, Tohamy HG, El-Sayed YS. Melatonin mitigates Thioacetamide-induced hepatic fibrosis via antioxidant activity and modulation of Proinflammatory cytokines and Fibrogenic genes. Life Sci. 2018;192:136-143. https://doi.org/10.1016/j.lfs.2017.11.036
3. Chilakapati J, Shankar K, Korrapati MC, Hill RA, Mehendale HM. Saturation toxicokinetics of thioacetamide: role in initiation of liver injury. Drug Metab Dispos. 2005;33:1877-1885. https://doi.org/10.1124/dmd.105.005520
4. Hajovsky H, Hu G, Koen Y, Sarma D, Cui W, Moore DS, Staudinger JL, Hanzlik RP. Metabolism and toxicity of thioacetamide and thioacetamide S-oxide in rat hepatocytes. Chem Res Toxicol. 2012;25:1955-1963. https://doi.org/10.1021/tx3002719
5. Ganesan K, Sukalingam K, Xu B. Solanum trilobatum L. Ameliorate thioacetamide-induced oxidative stress and hepatic damage in albino rats. Antioxidants(Basel). 2017;6:68. https://doi.org/10.3390/antiox6030068
6. Lassila V, Virtanen P. Influence of experimental liver injury on rat blood and alveolar bone under stress. Acta Anat(Basel). 1984;118:116-121. https://doi.org/10.1159/000145830
7. Nakano A, Kanda T, Abe H. Bone changes and mineral metabolism disorders in rats with experimental liver cirrhosis. J Gastroenterol Hepatol. 1997;11:1143-1154. https://doi.org/10.1111/j.1440-1746.1996.tb01843.x
8. Mirkova ET. Activities of the rodent carcinogens thioacetamide and acetamide in the mouse bone marrow micronucleus assay. Mutat Res. 1996;352:23-30. https://doi.org/10.1016/0027-5107(95)00169-7
9. Jamshidzadeh A, Heidari R, Abasvali M, Zarei M, Ommati MM, Abdoli N, Khodaei F, Yeganeh Y, Jafari F, Zarei A, Latifpour Z, Mardani E, Azarpira N, Asadi B, Najibi A. Taurine treatment preserves brain and liver mitochondrial function in a rat model of fulminant hepatic failure and hyperammonemia. Biomed Pharmacother. 2017;86:514-520. https://doi.org/10.1016/j.biopha.2016.11.095
10. Kang JS. Fluorescence detection of cell death in liver of mice treated with thioacetamide. Toxicol Res. 2018;34:1-6. doi: 10.5487/TR.2018.34.1.001. https://doi.org/10.5487/TR.2018.34.1.001
11. Schyman P, Printz RL, Estes SK, Boyd KL, Shiota M, Wallqvist A. Identification of the toxicity pathways associated with thioacetamide-induced injuries in rat liver and kidney. Front Pharmacol. 2018;9:1272. https://doi.org/10.3389/fphar.2018.01272
12. Johnell O, Kanis JA. An estimate of the worldwide prevalence and disability associated with osteoporotic fractures. Osteoporos Int. 2006;17:1726-33. https://doi.org/10.1007/s00198-006-0172-4
13. Compston JE, McClung MR, Leslie WD. Osteoporosis. Lancet. 2019;393:364-376. https://doi.org/10.1016/S0140-6736(18)32112-3
14. Stone KL, Seeley DG, Lui LY, Cauley JA, Ensrud K, Browner WS, Nevitt MC, Cummings SR, Osteoporotic Fractures Research Group. Osteoporotic Fractures Research, BMD at multiple sites and risk of fracture of multiple types: long-term results from the Study of Osteoporotic Fractures. J Bone Miner Res. 2003;18: 1947-1954. https://doi.org/10.1359/jbmr.2003.18.11.1947
15. Henriksen K, Neutzsky-Wulff AV, Bonewald LF, Karsdal MA. Local communication on and within bone controls bone remodeling. Bone. 2009;44:1026-1033. https://doi.org/10.1016/j.bone.2009.03.671
16. Matsuo K, Galson DL, Zhao C, Peng L, Laplace C, Wang KZQ, Bachler MA, Amano H, Aburatani H, Ishikawa H, Wagner EF. Nuclear Factor of Activated T-cells (NFAT) Rescues Osteoclastogenesis in Precursors Lacking c-Fos. J Biol Chem. 2004;279:26475-26480. https://doi.org/10.1074/jbc.M313973200
17. Fan F, Bashari MH, Morelli E, Tonon G, Malvestiti S, Vallet S, Jarahian M, Seckinger A, Hose D, Bakiri L, Sun C, Hu Y, Ball CR, Glimm H, Sattler M, Goldschmidt H, Wagner EF, Tassone P, Jaeger D, Podar K. The AP-1 Transcription factor JunB is essential for multiple myeloma cell proliferation and drug resistance in the bone marrow microenvironment. Leukemia. 2017;31:1570-1581. https://doi.org/10.1038/leu.2016.358

18. Biao W, Dingjun H, Zhen Z, Wenjie G, Hu P, Yuan X, Baorong H, Lingbo K. Inhibition effects of a natural inhibitor on RANKL downstream cellular signalling cascades cross-talking. J Cell Mol Med. 2018;22: 4236-4242. https://doi.org/10.1111/jcmm.13703
19. Rosen V. BMP2 signaling in bone development and repair. Cytokine Growth Factor Rev. 2009;20:475-480. https://doi.org/10.1016/j.cytogfr.2009.10.018
20. Virtanen P, Lassila V. Influence of thioacetamide-provoked liver injury on female rat blood and alveolar bone under stress. Acta Anat (Basel). 1986;127:285-289. https://doi.org/10.1159/000146299
21. Goswami S, Maity AC, Das NK. Advanced reagent for thionation: Rapid synthesis of primary thioamides from nitriles at room temperature. J Sulfur Chem. 2007;28:233-237. https://doi.org/10.1080/17415990701314069
22. Dyachenko VD, Krivokolysko SG, Litvinov VP. Synthesis of arylmethylenecyanothioacetamides in a Michael reaction. Mendeleev Commun. 1998;8:23-24. https://doi.org/10.1070/MC1998v008n01ABEH000816
23. El-Shwiniy WH, Sadeek SA. Synthesis and characterization of new 2-cyano-2-(p-tolyl-hydrazono)-thioacetamide metal complexes and a study on their antimicrobial activities. Spectrochim Acta A Mol Biomol Spectrosc. 2015;137:535-546. https://doi.org/10.1016/j.saa.2014.08.124
24. Mingzhang G, Min W, Qi-Huang Z. Synthesis of carbon-11-labeled imidazopyridine- and purine-thioacetamide derivatives as new potential PET tracers for imaging of nucleotide pyrophosphatase/phosphodiesterase 1 (NPP1). Bioorg Med Chem Lett. 2016;26:1371-1375. https://doi.org/10.1016/j.bmcl.2016.01.081
25. Peng Z, Xiao L, Zhenyu L, Xuwang C, Ye T, Wenmin C, Xinyong L, Christophe P, Clercq ED. Structure-based bioisosterism design, synthesis and biological evaluation of novel 1,2,4-triazin-6-ylthioacetamides as potent HIV-1 NNRTIs. Bioorg Med Chem Lett. 2012;22:7155-7162. https://doi.org/10.1016/j.bmcl.2012.09.062
26. Permuy M, López-Pea M, Muoz F, González-Cantalapiedra A. Rabbit as model for osteoporosis research. J Bone Miner Metab. 2019;37:573-583. https://doi.org/10.1007/s00774-019-01007-x
27. Soriano E, Marco-Contelles J. Mechanistic insights on the cycloisomerization of polyunsaturated precursors catalyzed by platinum and gold complexes. Acc Chem Res. 2009;42:1026-1036. https://doi.org/10.1021/ar800200m
28. Tsukamoto H. Development of new palladium(0)-catalyzed reactions based on novel oxidative addition mode. Yakugaku Zasshi. 2008;128:1259-1266. https://doi.org/10.1248/yakushi.128.1259
29. Mansour HM, Salama AAA, Abdel-Salam RM, Ahmed NA, Yassen NN, Zaki HF. The anti-inflammatory and anti-fibrotic effects of tadalafil in thioacetamide-induced liver fibrosis in rats. Can J Physiol Pharmacol. 2018;96:1308-1317. https://doi.org/10.1139/cjpp-2018-0338
30. Koblihová E, Mrázová I, Vernerová Z, Ryska M. Acute Liver Failure Induced by Thioacetamide: Selection of Optimal Dosage in Wistar and Lewis Rats. Physiol Res. 2014;63:491-503. https://doi.org/10.33549/physiolres.932690
31. Yogalakshmi B, Viswanathan P, Anuradha CV. Investigation of antioxidant, anti-inflammatory and DNA-protective properties of eugenol in thioacetamide-induced liver injury in rats. Toxicology. 2010;268: 204-212. https://doi.org/10.1016/j.tox.2009.12.018
32. Bashandy SAE, Alaamer A, Moussa SAA, Omara EA. Role of zinc oxide nanoparticles in alleviating hepatic fibrosis and nephrotoxicity induced by thioacetamide in rats. Can J Physiol Pharmacol. 2018;96:337-344. https://doi.org/10.1139/cjpp-2017-0247
33. Mladenović D, Krstić D, Colović M, Radosavljević T, Rasić-Marković A, Hrncić D, Macut D, Stanojlović O. Different sensitivity of various brain structures to thioacetamide-induced lipid peroxidation. Med Chem. 2012;8:52-8. https://doi.org/10.2174/157340612799278603
34. Parola M, Robino G. Oxidative stress-related molecules and liver fibrosis. J Hepatol. 2001;35:297-306. https://doi.org/10.1016/S0168-8278(01)00142-8
35. Lee YH, Son JY, Kim KS, Park YJ, Kim HR, Park JH, Kim KB, Lee KY, Kang KW, Kim IS, Kacew S, Lee BM, Kim HS. Estrogen deficiency potentiates thioacetamide-induced hepatic fibrosis in Sprague-Dawley rats. Int J Mol Sci. 2019;20:3709. https://doi.org/10.3390/ijms20153709

36. Zargar S, Wani TA, Alamro AA, Ganaie MA. Amelioration of thioacetamide-induced liver toxicity in Wistar rats by rutin. Int J Immunopathol Pharmacol. 2017;30:207-214. https://doi.org/10.1177/0394632017714175
37. Rock KL, Kono H. The inflammatory response to cell death. Annu Rev Pathol. 2008;3:99-126. https://doi.org/10.1146/annurev.pathmechdis.3.121806.151456
38. Akhtar T, Sheikh N. An overview of thioacetamide-induced hepatotoxicity. Toxin Reviews. 2013;32:43-46. https://doi.org/10.3109/15569543.2013.805144
39. Seeman E. Age- and menopause-related bone loss compromise cortical and trabecular microstructure. J Gerontol A Biol Sci Med Sci. 2013;68:1218-25. https://doi.org/10.1093/gerona/glt071
40. Yamada M, Chen C, Sugiyama T,. Kim WK. Effect of age on bone structure parameters in laying hens. Animals(Basel). 2021;11:570. https://doi.org/10.3390/ani11020570
41. Jingjing L, Zhuanzhuan Z, Qi G, Yanhong D, Qipeng Z, Xueqin M. Syringin prevents bone loss in ovariectomized mice via TRAF6 mediated inhibition of NF-kappaB and stimulation of PI3K/AKT. Phytomedicine. 2018;42:43-50. https://doi.org/10.1016/j.phymed.2018.03.020
42. Nussler AK, Wildemann B, Freude T, Litzka C, Soldo P, Friess H, Hammad S, Hengstle JG, Braun KF, Trak-Smayra V, Godoy P, Ehnert S. Chronic CCl4 intoxication causes liver and bone damage similar to the human pathology of hepatic osteodystrophy: a mouse model to analyse the liver-bone axis. Arch Toxicol. 2014;88:997-1006. https://doi.org/10.1007/s00204-013-1191-5
43. Luu HH, Song WX, Luo X, Manning D, Luo J, Deng ZL, Sharff KA, Montag AG, Haydon RC, He TC. Distinct roles of bone morphogenetic proteins in osteogenic differentiation of mesenchymal stem cells. J Orthop Res. 2010;25:665-677. https://doi.org/10.1002/jor.20359
44. Al-Bari MAA, Hossain S, Mia U, Mamun MAA. Therapeutic and mechanistic approaches of tridax procumbens flavonoids for the treatment of osteoporosis. Curr Drug Targets. 2020;21:1687-1702. https://doi.org/10.2174/1389450121666200719012116
45. Halloran D, Durbano HW, Nohe A. Bone Morphogenetic Protein-2 in Development and Bone Homeostasis. J Dev Biol. 2020;8:19. https://doi.org/10.3390/jdb8030019
46. Song I, Kim JH, Kim KK, Jin HM, Youn BU, Kim N. Regulatory mechanism of NFATc1 in RANKL-induced osteoclast activation. Febs Lett. 2009;583:2435-40. https://doi.org/10.1016/j.febslet.2009.06.047
47. Youn-Hwan H, Hyunil H, Rajeong K, Chang-Won C, Young-Ran S, Hee-Do H, Taesoo K. Anti-osteoporotic effects of polysaccharides isolated from persimmon leaves via osteoclastogenesis inhibition. Nutrients. 2018;10:901. https://doi.org/10.3390/nu10070901
48. Virtanen P, Lassila V. Influence of thioacetamide-provoked liver injury on female rat blood and alveolar bone under stress. Acta Anat (Basel). 1986;127:285-9. https://doi.org/10.1159/000146299